Tinaut Fluixa, FV.; Reyes, M.; Giménez, B.; Pastor Soriano, JV. (2011). Measurements of OH* and CH* Chemiluminescence in Premixed Flames in a Constant Volume Combustion Bomb under Autoignition Conditions. ENERGY & FUELS. 25:119-129. doi:10.1021/ef1013456.

Measurements of OH* and CH* chemiluminescence in premixed flames in a constant volume combustion bomb under autoignition conditions

F.V. Tinaut[1], M. Reyes[1], B. Giménez[1] and J.V. Pastor[2]*

[1] Department of energetic and fluid-mechanics engineering, University of Valladolid, Paseo del Cauce, 59, 47011, Valladolid – SPAIN

[2] CMT-Motores Térmicos, Universidad Politécnica de Valencia, Camino de Vera, s/n, 46022, Valencia – SPAIN

* miriam.reyes@uva.es

RECEIVED DATE

ABSTRACT.

The objectives of this paper are: (1) to parametrically study OH* and CH* chemiluminescence traces evolution as a function of initial pressure, temperature and equivalence ratio of premixed flames of n-heptane, under autoignition conditions, in a constant volume combustion bomb. The signals of the electronically excited states of OH* (306 nm) and CH* (430 nm) have been detected through band-pass filters with two photo-multiplier tubes placed in an optical access of the combustion bomb.

(2) To determine the feasibility of using OH* and CH* chemiluminescence signals as active-control parameters for premixed flames. For this purpose, a correlation between OH* chemiluminescence emissions and the equivalence ratio and the rate of heat release during the combustion process is

obtained, as well as a correlation between CH* chemiluminescence emissions and the adiabatic flame temperature. (3) To investigate the relationship between the OH* and CH* chemiluminescent emissions in premixed combustions of n-heptane, iso-octane and a mixture of 50% of n-heptane and 50% of toluene and the equivalence fuel/air ratio, for given initial temperature and pressure.

To reach these objectives, measurements of OH* and CH* chemiluminescences from premixed flames of n-heptane with autoignition are reported at equivalence ratios ranging from 0.8 to 1.0, in a constant volume combustion bomb. The morphology of the curves and the relationships with parameters of interest during the combustion process (i.e. the rate of heat release, burned temperature …) are studied.

In addition premixed combustions of iso-octane, n-heptane and a mixture of n-heptane and toluene are also investigated at different fuel/air equivalence ratios for a given initial pressure and temperature, to asses the possibility of using the ratio between the OH* and CH* chemiluminescence signals to monitorize the equivalence ratio during the combustion, as other authors have considered before.

1. Introduction

Chemiluminescence from hydrocarbon flames arises from specific molecules that are lifted to an excited state by exothermic chemical reactions and then subsequently decay back to equilibrium energy levels by emitting a photon. Chemiluminescence emission occurs in specific wavelength bands that are characteristic of the emitting molecules. Since the molecules responsible for the chemiluminescence change for different combustion regimes and types, chemiluminescent emissions can provide information about the nature of the reactions and the fuel/air mixture[1]. This emission results primarily from CH*, OH*, C_2* and CO_2*, with weaker emissions from HCO*, CO* and CH_2O* (where * denotes an electronically excited state). As chemiluminescence is produced directly by exothermic chemical reactions, it marks the location of the initial reactions, during the combustion processes, with the limitation that the signal collects the total emission along the line of sight, and is thus not spatially resolved (it is only temporally resolved).

This work is focused on the interpretation of OH* and CH* chemiluminescence data, since they have been widely employed as a flame marker[2] to study the combustion process by spectral combustion diagnostics.[1,3,4,5,6,7,8]

In previous works, the OH* maximum peak value was found to be well correlated with the rate of heat release[9], so that it could be used as a measurement tool; OH* and CH* chemiluminescence can provide data on the flame front region and the structure of the flame front can be characterized by the duration of the chemiluminescence emissions.[10] CH* have also been used to study the autoignition process in Diesel engines.[11,12] One of the main advantages of using chemiluminescence for combustion diagnostics is its relation with the equivalence ratio during the combustion process. Several researchers have found a connection between the chemiluminescence intensity and the local equivalence ratio[4,13-19], which is an important parameter in diagnostic and control processes.

Some of the pioneer works, developed by Clark et al.[20,21], studied the chemiluminescence emitted during combustion in a spark ignition internal combustion engine and concluded that the intensity of each radical depends on the fuel properties and the initial equivalence ratio. CH* and C_2* chemiluminescence were found to be good indicators of the local equivalence ratio, and the radicals OH* and CO_2* had their maximum peak of emission near the point at which maximum laminar combustion velocity were reached. Dandy and Vosen[19] made a numerical and experimental study of the OH* chemiluminescence in methane flames. The experimental study was carried out in a cylindrical combustion bomb with an optical access to detect the OH* in 306 nm. Their results showed a fair correlation between the OH* chemiluminescence detected and the local equivalence ratio. The work by Docquier et al.[22], on combustion of methane in a Bunsen burner, confirms the conclusions of the previous work that chemiluminescence of OH*, CH* and C_2* is a good indicator of the local equivalence ratio inside the burner. Higgins et al.[13] performed a study about the OH* and CH* chemiluminescence emissions produced in a Bunsen burner using methane. They found a relation between the OH*/CH* ratio and the equivalence ratio, and thus, this rate can be used to evaluate the local equivalence ratio in flames. In a following work developed by Higgings et al.[18], they completed their previous work by studying the OH* chemiluminescence from premixed methane flames at elevated pressures and different equivalence ratios. They found a correlation between the chemiluminescence emissions, the pressure and the equivalence ratio. Docquier et al.[4] developed a system to control the equivalence ratio in a burner by using chemiluminescence emissions, once the correlation between chemiluminescence and equivalence ratio was confirmed.

Chemiluminescence emissions have also been used in internal combustion engines[17] and correlations between the CH*/OH* and C_2*/OH* ratios and the equivalence ratio have been obtained. Other studies developed in different burners[14] and in turbines[7] obtained the same conclusion.

Price et al.[23] used CH* and C_2* chemiluminescence emissions to study noise during combustion. They concluded that there was a direct relation between the emissions detected and the mass flow rate, and

thereby the pressure inside the burner. The works by Clark[21] and Price et al.[23] can be considered as the first evidences of the relationship between the RoHR and the chemiluminescence emissions inside the combustion chamber. Since then, several studies have been developed in different experimental facilities, confirming the correlation between the RoHR and the chemiluminescence emitted by chemical radicals, which are important during the combustion process. For this reason, it is generally accepted that OH*, CH* and C_2* chemiluminescence give a measure of the global heat released by a flame.

Chemiluminescence has also been used for studying knock in spark ignition engines and engines running in HCCI mode. One pioneer work on the study of knock is that developed by Withrow and Rassweiler[24], which described the chemiluminescence emitted in a spark ignition engine by separating it in two parts: flame front and *afterglow*, each with its characteristic emissions. They concluded that the chemical reactions during the knock process are different to those produced during the normal or conventional combustion.

In the case of HCCI-type combustion, Hultqvist et al.[25] made a study of the chemiluminescence generated in this combustion inside a compression ignition engine.

Henceforth, multiple research works have proved that chemiluminescence emitted by chemical radicals in flames can be used (quantitatively and qualitatively) as a diagnostic tool[12,26,27], for combustion in internal combustion engines, burners, turbines and other combustion facilities. Dubreuil et al.[28] examines the effect of exhaust gas recirculation on the HCCI combustion of h-heptane in a transparent monocylinder diesel engine by visualizing the OH* natural emissions. Mancaruso et.al. [29] investigated the HCCI combustion using digital imaging and spectroscopic techniques to detect the presence of different radicals (OH, CH, HCO and CO) during the different processes of the HCCI combustion. In other work[30] they studied the HCCI combustion fuelled with a biofuel using optical measurements. They registered OH and HCO radicals during the combustion and found that OH was responsible of the NO formation inside the combustion chamber.

This paper is focused on the study of the OH* and CH* chemiluminescence emitted by the autoignition of n-heptane under different initial conditions of pressure, temperature and equivalence fuel/air ratio. The fuel, n-heptane, has been chosen because it is considered a Diesel surrogate[31], which simulates the cetane number of the Diesel fuel.

First, the morphology of the OH* and CH* chemiluminescence curves obtained in a combustion bomb is described: The temporal evolution of the chemiluminescence curves is presented, analyzed and discussed as a function of the equivalence ratio, the initial pressure and the temperature. Following this, we show certain relationships between the chemiluminescent emissions and important parameters during the combustion process, like the rate of heat release, the flame temperature and the burning velocity.

The interest of the OH* chemiluminescence to identify the RoHR and equivalence ratio (Fr), when combined with CH* chemiluminescence, is then analyzed in n-heptane, iso-octane and a mixture of n-heptane and toluene flames for varying initial pressure and temperature: (i) n-heptane; (ii) a mixture of 50% n-heptane and 50% toluene, which is a Diesel fuel surrogate because the n-heptane simulates the Diesel cetane number and the toluene represents the aromatic content; and (iii) iso-octane, which reproduces the octane number of the conventional gasoline, and can be considered a gasoline surrogate.

In the final section, the investigation is summarized and conclusions are drawn.

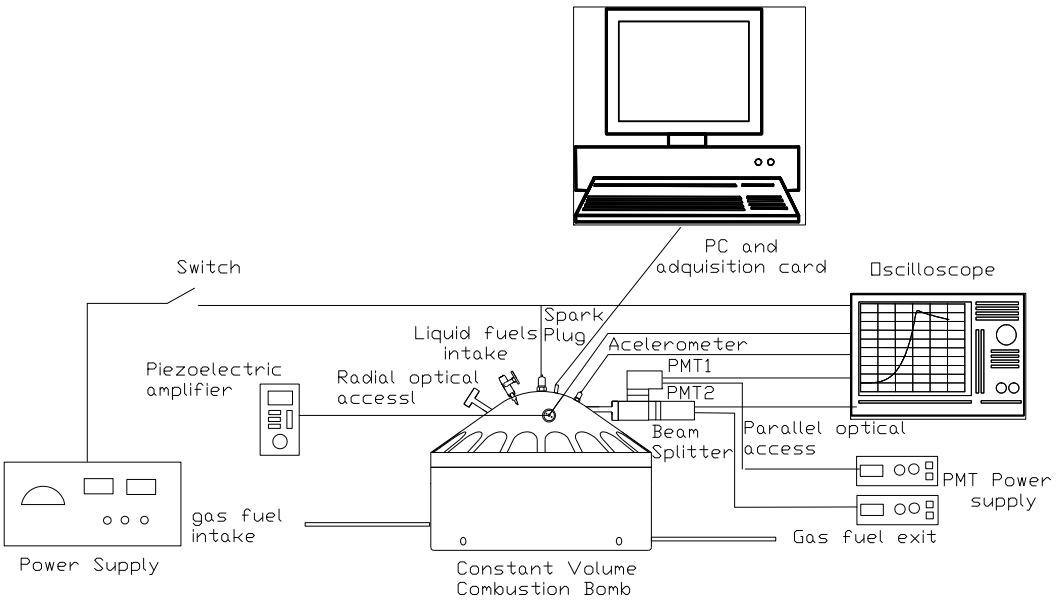

(i). Scheme of the experimental setup

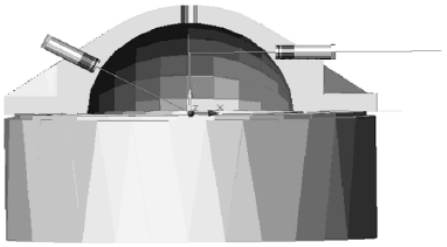

(ii) Sketch of the optical accesses

Fig. 1. Experimental facility

2. Experimental setup

2.1. Experimental facility and control of the test conditions

The experimental setup used in this work consists of a test facility designed for the study and characterization of the gaseous and liquid fuel combustion processes. The main components are a *constant volume combustion bomb* (CVCB), a *measurement system* and a complete *equipment for the introduction of fuels*. In Fig. 1i, a scheme of the experimental setup can be seen. The CVCB is a stainless steel spherical cavity of 0.2 meters diameter, with two optical accesses to detect the chemiluminescence emitted by the excited chemical radicals during the combustion process. One optical access is radial pointing at the centre of the CVCB and the second is horizontal and points to the outer region of the combustion chamber near the wall. A sketch is shown in Fig. 1ii. The CVCB has been designed to resist pressures of up to 40 MPa and temperatures of up to 1073 K during the development of the combustion. There are two electrodes inside the CVCB to ignite the mixture and start combustion at the geometric centre of the sphere.

Before the start of the combustion initial condition of pressure are fixed by using three piezoresistive transducers (with three different ranges of measuring). A thermocouple, a PID controller and four thermal resistors (with 1.25 kW each one) are used to heat the sphere and fix the initial temperature of the fuel/air mixture. Compressed air is introduced inside the CVCB through the gas intake, while liquid fuels are introduced by means of a manual valve placed at the top of the sphere with three Hamilton syringes (with different capacities) for a finest precision liquid measuring and needles with 0.2 meters of longitude to guarantee the introduction of all the fuel, once the vacuum is made in the CVCB.

Thermodynamic conditions of the unburned mixture prior to autoignition are controlled indirectly, by fixing the initial conditions of pressure, temperature and fuel/air ratio before generating the spark. Then,

real conditions at the moment of autoignition are estimated from the analysis of the pressure trace inside the chamber by means of a two-zone combustion model.[32]

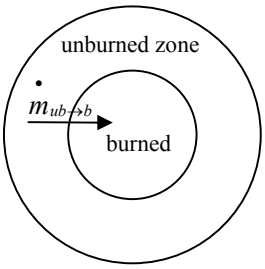

Fig 2. Diagnosis model outline.

This model considers two different zones in the combustion chamber, for burned and unburned gases respectively (see the scheme of Fig. 2), and applies the energy, volume and mass conservation and ideal gas equations in each zone to calculate the temperature in each zone, the laminar burning velocity, the burned mass fraction and other important parameters.[33,34] The main inputs for the model[32] are the experimental pressure traces and the initial data of fuel composition and the total mass within the CVCB.

Note that after the autoignition of the mixture the results provided by the model are only an approximation.

Additionally to the calculation of the burned mass fraction by the two-zone combustion model described above, the RoHR is calculated based on the First Law of Thermodynamics for a quasi static system i.e. with uniform pressure and mean temperature at any instant in time, see Eqs. 1 and 2:

$$\frac{dQ}{dt} = \frac{1}{\gamma - 1} V \frac{dp}{dt} \qquad (1)$$

where γ is the mean adiabatic coefficient. Then the RoHR is

$$RoHR = \frac{dQ/dt}{m_f H_f} \quad (2)$$

Hydroxyl radical cheluminescence results from the emission of light from electronically excited hydroxyl radicals (OH*). OH* is produced in the first electronically excited state and the transition $^2\sum^+ \rightarrow {}^2\Pi$ may be observed at the 305.4 nm band of OH[1]. The most likely hydroxyl producing reactions result in electronic ground state OH.

In general, it is accepted that OH* chemiluminescence emission in the flame is produced as OH $_A{}^2\sum$ by oxidation of CH[3], see eq (3).

$$CH + O_2 = CO + OH^* (^2\sum^+) \quad (3)$$

This mechanism was proposed by Krishnamachari et al.[35] and it has been utilized frequently since then, because this reaction is one of the most likely for the production of OH*($^2\sum^+$) radicals. These OH* radicals have a rotational energy distribution, typical of systems which are not in equilibrium.[36]

Hydroxyl radicals exist both in the flame front and in hot post-combustion gases and, thus, are best detected by using techniques such as absorption, laser induced fluorescence or chemiluminescence.[37]

CH* chemiluminescence near 430 nm is from excited state CH* (CH($A^2\Delta$)) produced primarily through the reaction of C_2H with molecular oxygen.[3, 38]:

$$C_2H + O (^3P) \rightarrow CH^* (A^2\Delta) + CO \quad (4)$$

In flames of low pressure combustions, eq. (4) is the most representative. However, for rich flames it is necessary to consider another mechanism of CH* production (see eq. (5)) to take into account the decomposition of the HCO* radical and the peroxide formation.[1]

$$CH + CO + H \Leftrightarrow CH^* + H_2O \quad (5)$$

The resulting excited OH* and CH* lose their energy either through spontaneous fluorescence (chemiluminescence) or through physical quenching (collisions).

2.2. Measurement methodology

During the combustion development pressure and OH* and CH* chemilumescence are directly measured. Two Hammamatsu 9536 photomultipliers (PMTs) are used for the detection of the chemiluminescence emitted by OH* and CH* radicals at 306 nm and 430 nm, respectively.[1] Radiation is collected through the optical access fused silica windows of the CVCB, a beam splitter and a group of pass-band optical filters centred at the required wavelengths.

The OH* chemiluminescence signal is measured by one of the photomultiplier tubes with a band-pass interference filter centred at 307.1 nm (25 nm FWHM) and 21% maximum transmission.

To measure CH* chemiluminescence, another PMT is used in combination with a band-pass interference filter centred at 430.0 nm with a full width at half maximum of 10 nm and 10 % of maximum transmission.

The time-resolved signals from the PMTs were recorded by a data acquisition system which consists of a digital oscilloscope and a computer board for data collection. Much care was taken to shield all cables and reduce the noise of the signals. In all results shown in this paper, OH* and CH* chemiluminescence signals were detected through the horizontal optical access, placed at 85 mm above the CVCB center.

Chemiluminescence is measured in lumens (lm or better nlm-10^{-9} lm), and the conversion factor is obtained with the correlation curve of the PMTs as a function of the input voltage.

A piezoelectric pressure transducer (Kistler type 7063) located at the wall of the CVCB registers the pressure in the chamber during combustion.

The temperature, burning velocity, burned mass fraction and other parameters during the combustion are obtained by using the two zone analysis model explained above.

More details of the experimental installation and measurement methodology can be seen in.[31]

2.3. Experimental procedure for thermodynamic conditions control

Once, the spark plug starts the combustion, a flame front propagates spherically across the combustion chamber increasing pressure and temperature in the chamber, and consequently also in the unburned fuel/air mixture. As the pressure and temperature increase enough as a consequence of flame propagation, they may cause autoignition of the still unburned mixture ahead of the flame front, in the outer regions of the combustion bomb. Otherwise, a conventional premixed combustion takes place inside the CVCB. As explained later, if autoignition takes place, it can progress either smoothly as in an HCCI engine, or lead to knock.

The chemiluminescence emissions during combustion can be divided in two different parts: flame front emissions and afterglow[24]. The flame front emissions consist of, mainly, OH*, CH* and C_2* radicals at specific wavelengths. Afterglow emissions are characterized by a continuous emission produced during the post-combustion process of the CO in CO_2[39,40]:

$$CO+1/2O_2 \rightarrow CO_2+h\upsilon \quad (6)$$

Thus a continuous emission between 300 and 600 nm is obtained along with the CO_2 (see, Eq. (6)).

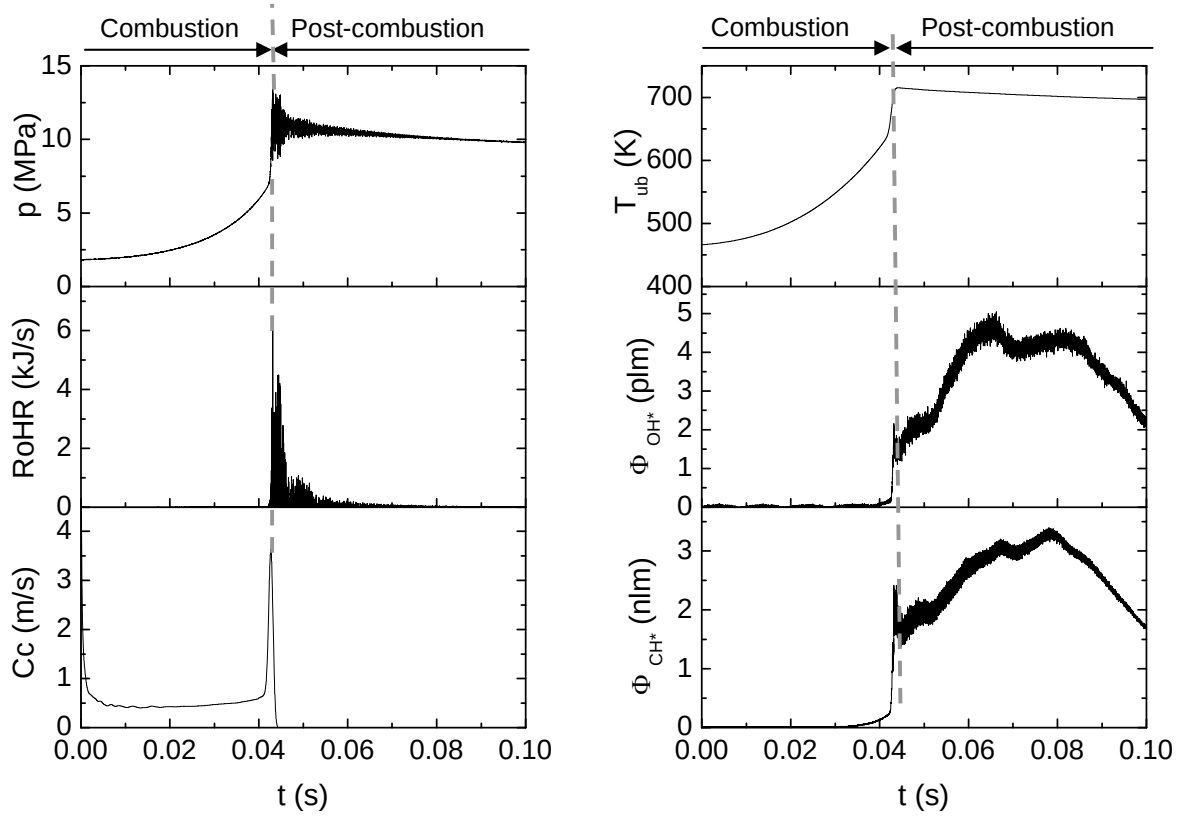

(i) Example of pressure, rate of heat release and combustion velocity

(ii) Example of temperature, OH* and CH* chemiluminescence emissions

Fig. 3 .Examples of some parameters obtained for a stoichiometric combustion of n-heptane with autoignition. Distinction between the combustion and the post-combustion (afterglow) zones.

The shape of the pressure and the chemiluminescence curves obtained in combustions with autoignition can be seen in Fig. 3, where the temporal evolution of the pressure and the OH* chemiluminescence emissions are plotted. In the pressure curve, a strong increment of the curve slope can be appreciated due to the autoignition process, followed by some ripples, due mainly, to the intensity of the autoignition process. The OH* and CH* chemiluminescence curves (see, Fig. 3ii) show a considerable rise at the beginning of the combustion, until a peak is obtained (which coincides with the autoignition point in the pressure curve), which is followed by a low fall and by another increment

which is followed by the higher value of the curve. The first peak is produced by the OH* radical emissions during the combustion process, while the second appears during the post-combustion process of the CO in CO_2.

In the present work, we focus on the study of the OH* and CH* chemiluminescence emissions produced during the combustion process. For this reason we do not take into consideration the chemiluminescence emitted during the post-combustion process.

The abruptness of the autoignition event can be described through the *intensity of the autoignition* parameter, which can be defined as the increment of the pressure, as a consequence of the autoignition of the fresh mixture observed in the pressure curve (see Fig. 4).

$$Int_{aut} = p_{\max} - p_{after.aut} \tag{7}$$

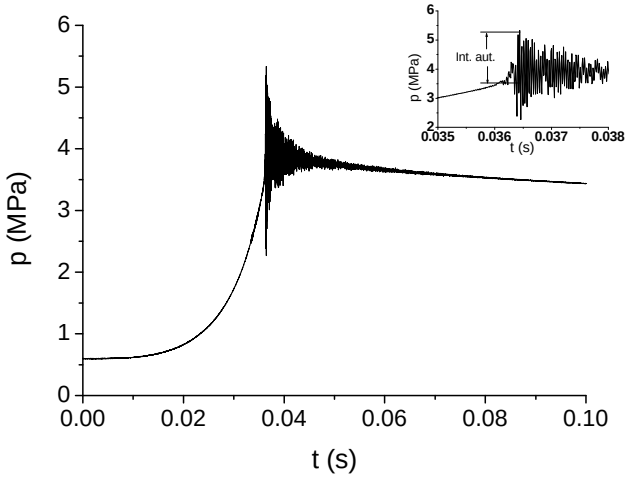

Fig. 4. Autoignition intensity definition in a curve of stoichiometric n-heptane autoignition with pi=1.8 MPa and Ti=463K

3. Results and discussion

In this section we will study the chemiluminescence curves obtained in combustions of n-heptane with autoignition in the CVCB to examine the influence of the equivalence ratio, initial temperature and pressure on the morphology of the chemiluminescence curves. In a second part, we will asses the relation between the rate of heat release and the OH* chemiluminescence. And finally, we will analyse premixed combustion of n-heptane, iso-octane and a mixture of n-heptane and toluene (without autoignition) to verify the relationship between the equivalence ratio and the OH*/CH* chemiluminesce ratio.

3.1. Experimental design

The experimental design utilized to develop the experiments with the n-heptane fuel, under autoignition conditions, for three different equivalence ratios of 1, 0.9 and 0.8, consists of a D-optimal design of third order. This design proposes to carry out eighteen experiments for the autoignition of stoichiometric n-heptane, seventeen for the autoignition of n-heptane with equivalence ratio of 0.9, and sixteen for the autoignition of n-heptane with 0.8 of equivalence ratio. The initial conditions of pressure and temperature of the experiments proposed appear in Fig. 5, where the standard deviation of the out variables by testing only in the proposed points of the autoignition area is also plotted.

Once we have the information about the combustion process (RoHR, flame temperature, combustion velocity, among others), it is possible to obtain some relations with the chemiluminescent emissions.

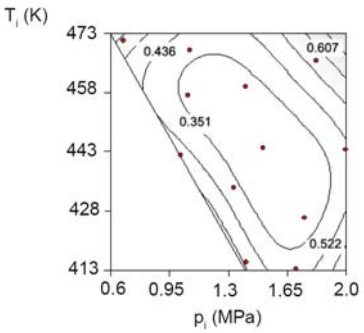

(i) Fr=1

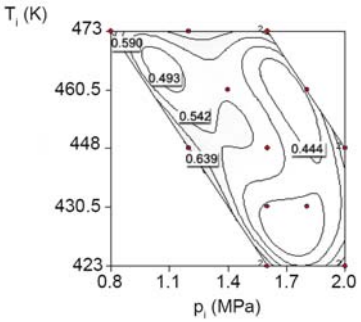

(ii) Fr=0.9

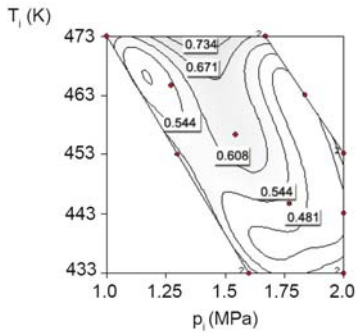

(iii) Fr=0.8

Fig. 5. Standard deviation of the experimental design proposed by a D-optimal type design of the n-heptane autoignition at different equivalence ratios 1, 0.9 and 0.8.

3.2. Influence of equivalence ratio, temperature and pressure on the chemiluminescence curves development

In order to study the morphology of the OH* and CH* chemiluminescence curves, we will examine the effect of the equivalence ratio, the initial temperature and the initial pressure, separately for n-heptane/air mixtures autoignition.

3.2.1. Effect of equivalence ratio

In Fig. 6, the temporal evolution of the OH* (Fig. 6i) and CH* (Fig. 6ii) chemiluminescence on n-heptane combustions with autoignition are plotted for different equivalence ratios, for a given initial pressure and temperature of 2.0 MPa and 443 K, respectively.

There are several trends in Fig. 6:

(1) A little change in the equivalence ratio (from 0.8 to 0.9 or from 0.9 to 1.0) gives a notable increase in the intensity of OH* chemiluminescence (by a factor of 10, approximately). However, the same change in the equivalence ratio only produces a weak increase of CH* chemiluminescence. That means that OH* chemiluminescence is more dependent on the equivalence ratio of the mixture and, therefore, on the quantity of fuel inside the initial mixture.

(2) This increment in the OH* and CH* chemiluminescence can be associated to an effect of the combustion temperature. An increase in the equivalence ratio towards stoichiometry increases the adiabatic flame temperature.[33]

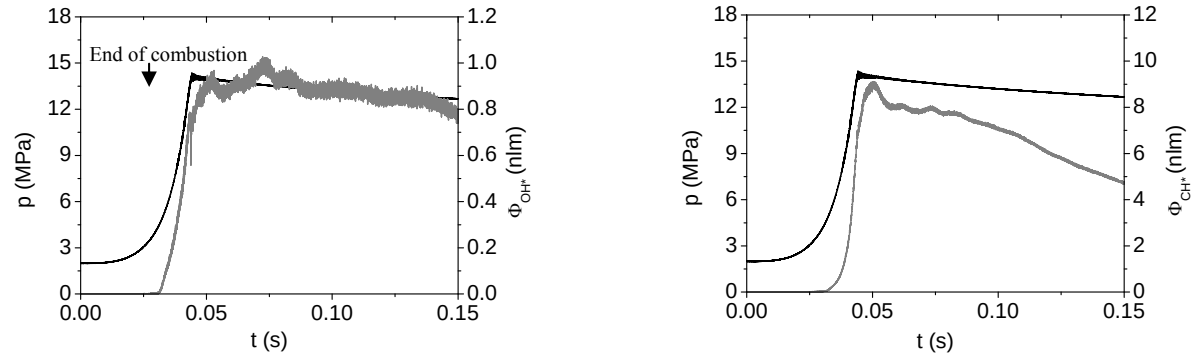

(i) Fr = 1

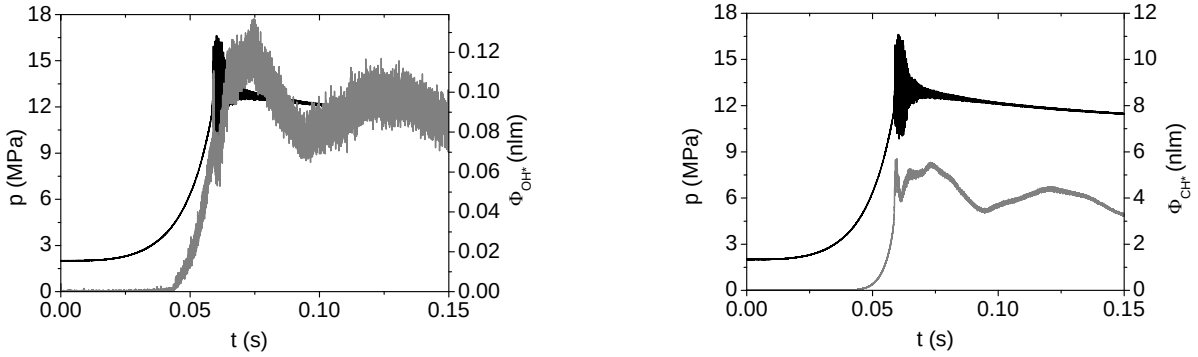

(ii) Fr = 0.9

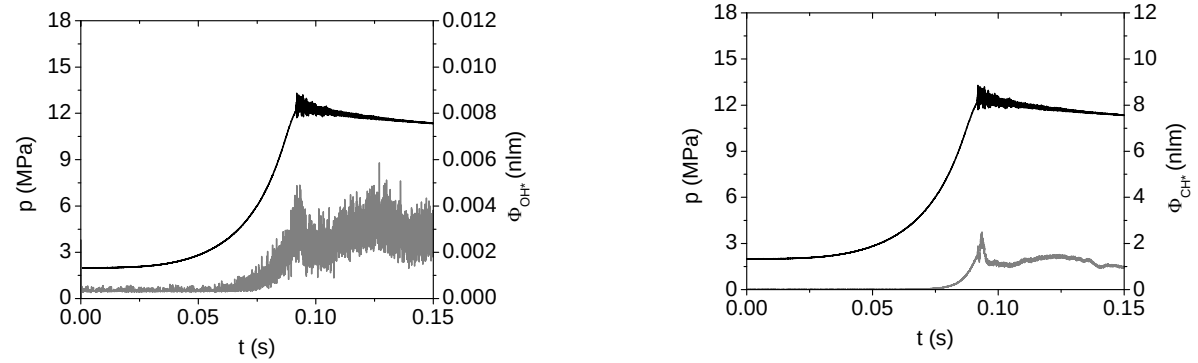

(iii) Fr = 0.8

Fig. 6. Temporal evolution of the pressure (black line), OH* (grey line in the left plots) and CH* (grey line in the right curves) chemiluminescence in n-heptane premixed combustions with autoignition, for different equivalence ratios and for a fixed initial pressure and temperature of 2.0 MPa and 443 K, respectively.

(3) CH* chemiluminescence is more intense than OH* chemiluminescence and the values are different for each equivalence ratio considered. In fact, for lean mixtures (equivalence ratios of 0.8 and 0.9) CH* chemiluminescence is 1000 and 100 times, respectively, bigger than OH* chemiluminescence. However, for stoichiometric mixtures (equivalence ratio of 1.0) the CH* chemiluminescence is only 10 times bigger than the OH* chemiluminescence). This can be explained by the fuel used (n-heptane) which has a high level of carbon and the CH* radical is the most predominant in the combustions. In other research work[9], developed with producer gas in stoichiometric conditions, the OH* and CH* chemiluminescence emissions are of the same magnitude order, which means that, the intensity of these emissions is very dependent on the fuel employed.

3.2.2. Effect of initial temperature and pressure

OH* chemiluminescence emissions

The morphology of the OH* chemiluminescence curves is shown in Fig. 7, as a function of the initial pressure and temperature, for a given equivalence ratio (in this case stoichiometric). The mean trends of these figures are the following: (1) There are two different shapes in the curves, the shapes of the curves for the lower temperatures (413 K and 443 K), and the shape of the curves for the highest temperature (473 K). The main difference between these two groups of curves is due to the initial temperature of each of the combustions. In the case of 473 K (the temperature is close to the spontaneous autoignition of the fuel, 493 K for n-heptane), the curves have a big peak which is very pronounced at the point at which the autoignition of the fuel is produced. The autoignition in this case is more abrupt because the quantity of the autoignited unburned mixture is bigger. This kind of autoignition is similar to the knock process in spark ignition engines (see Withrow and Rassweiler[24]) where the emissions from the radicals during the knock process are described: CH* emissions decreased considerably and the afterglow

disappeared, which is exactly the same that happens in the curves shown with the highest initial temperature.

The other group of curves has a less appreciable increment, as the combustion is propagated inside the CVCB. The curves reached a maximum near the point at which the maximum pressure is reached, in the main combustion (see the pressure curve), and this maximum is followed by an increment due to the afterglow emission in the post-combustion process.[33] Other authors have observed these emissions in the post-combustion processes. This type of autoignition process is smoother and more homogeneous than the knock type and it is similar to the autoignition produced in internal combustion engines running in HCCI-mode (homogeneous charge compression ignition).

(2) In general, for a given initial temperature, as the initial pressure grows, OH* chemiluminescence increases too, (see Fig. 7).

(3) For a given initial pressure, the trend with the increment of the initial temperature is ambiguous (see Fig 7). For the higher pressure (2.0 MPa) an increment in the initial temperature produces an increment in the chemiluminescence detected. When the pressure is 1.4 MPa, the maximum values of the chemiluminescence detected are similar and the shape of the curve only differs because the emissions at higher initial temperatures are generated at an earlier time, because the velocity of the combustion is more elevated. In the case of 1.0 MPa of initial pressure, we can see that the tendency with the increment of the initial temperature is to increase the chemiluminescence detected, with the exception of the curve at 473 K which has a different shape.

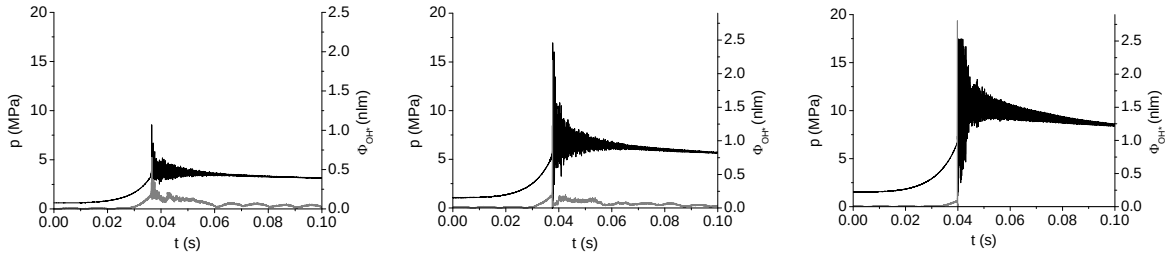

T_i = 473 K

p_i = 0.6 MPa p_i = 1.0 MPa p_i = 1.5 MPa

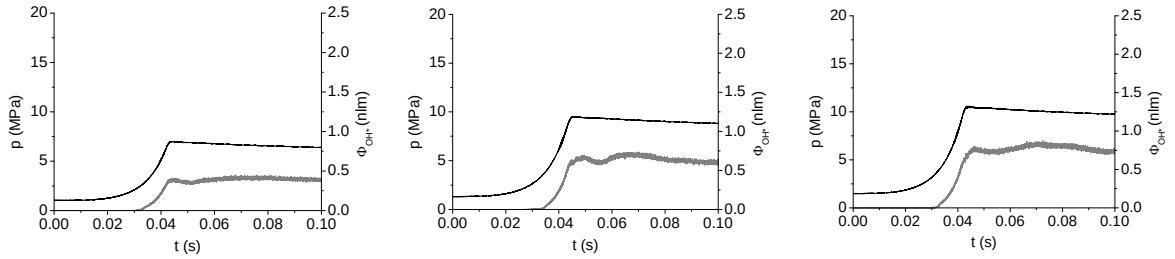

T_i = 443 K

p_i = 1.0 MPa p_i = 1.3 MPa p_i = 1.5 MPa

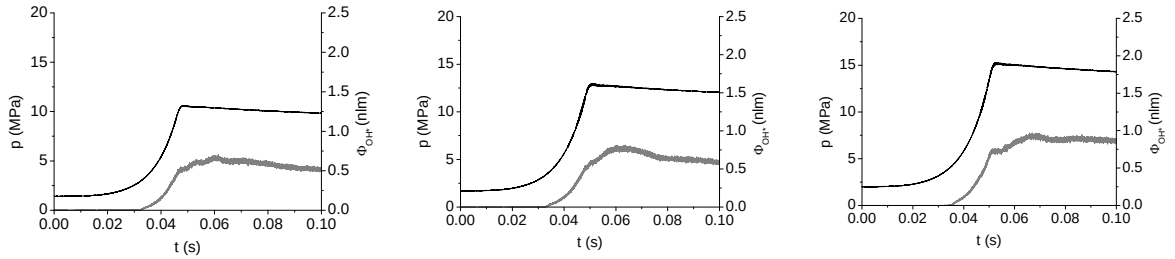

T_i = 413 K

p_i = 1.4 MPa p_i = 1.7 MPa p_i = 2.0 MPa

Fig. 7. Pressure curve (black line) and OH* chemiluminescence (grey line) in n-heptane combustions with autoignition event, for different initial pressures and temperatures, for a fixed stoichiometric equivalence ratio.

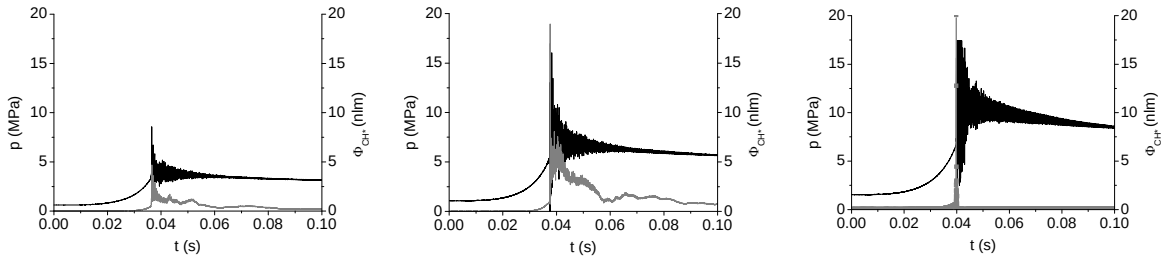

T_i = 473 K

p_i = 0.6 MPa p_i = 1.0 MPa p_i = 1.5 MPa

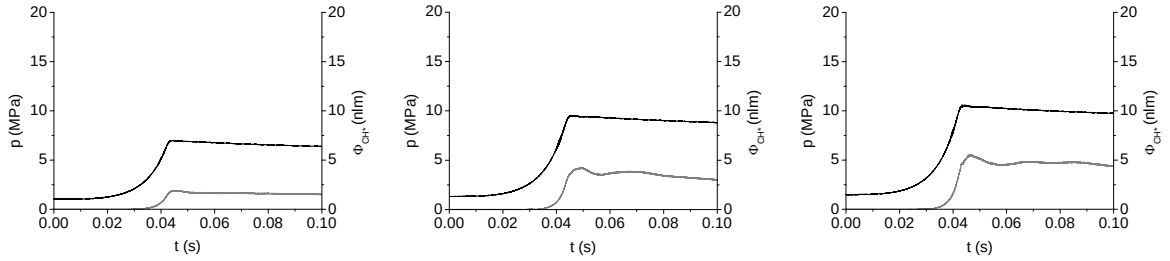

T_i = 443 K

p_i = 1.0 MPa p_i = 1.3 MPa p_i = 1.5 MPa

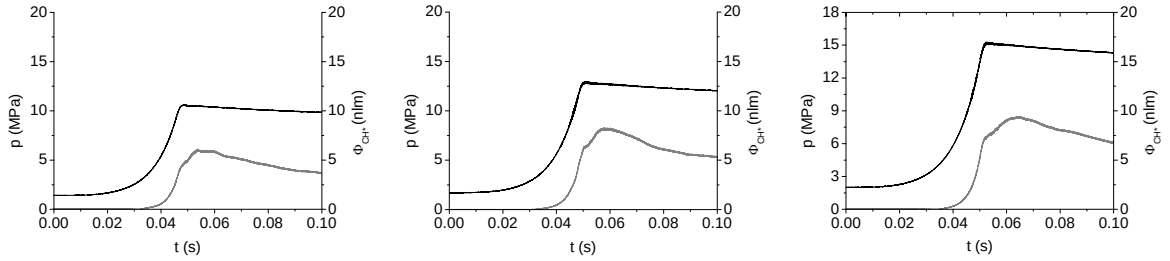

T_i = 413 K

p_i = 1.4 MPa p_i = 1.7 MPa p_i = 2.0 MPa

Fig. 8. Pressure curve (black line) and CH* chemiluminescence (grey line) in n-heptane combustions with autoignition event, for different initial pressures and temperatures, for a fixed stoichiometric equivalence ratio.

CH* chemiluminescence emissions

The trends of the CH* chemiluminescence (see Fig. 8) are similar to the OH* ones: (1) the shapes of the curves are again different, depending on the initial temperature considered (as happened with the OH* chemiluminescence). (2) For a given initial temperature, an increment in the initial pressure produces a rise in the chemiluminescence detected. (3) The trend with the growth of the initial temperature is the increment of the radiation detected, without taking in account the curve at 473 K, for the reason explained above.

In summary, the most influential parameter in the chemiluminescence curves morphology is the equivalence ratio, followed by the initial temperature and the initial pressure.

3.3. Relationship between the RoHR and OH* chemiluminescence

The time at which the maximum rate of heat release ($t_{RoHRmax}$) is reached is presented in Fig. 9 against the time of the maximum OH* chemiluminescence ($t_{OH^* max}$) for the experiments performed for three different equivalence ratios.

It is possible to see that, for lean equivalence ratios, the RoHR and the OH* chemiluminescence maximum are achieved at the same time, which means that a linear relation exists between them.

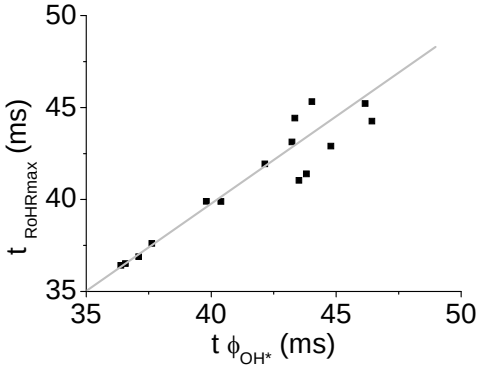

(i) Fr=1

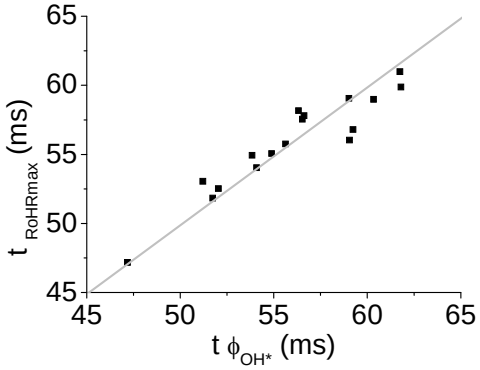

(ii) Fr=0.9

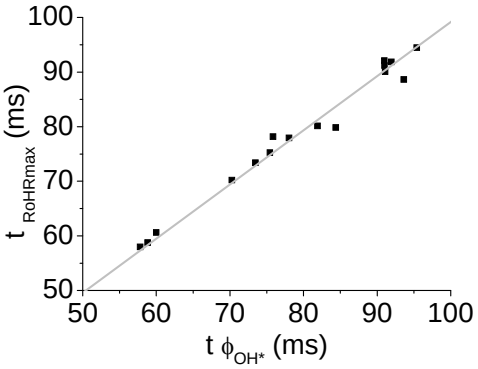

(iii) Fr=0.8

Fig. 9. Maximum Rate of Heat Release time and maximum OH* chemiluminescence emissions in combustions of n-heptane with autoignition for different equivalence ratios, initial pressures and temperatures.

3.4. Relationship between the equivalence ratio and the OH*/CH* ratio

Higgins et al.[7] found a relationship between the OH*/CH* chemiluminescence ratio and the equivalence ratio of the mixture for methane. With that relationship they were able to check the fuel/air equivalence ratio in combustors. In that relation, the rate of chemiluminescences had a quadratic dependence on the equivalence ratio.

In the present work, we try to find some relation between the ratio of chemiluminescences and the equivalence ratio for premixed combustions carried out inside the CVCB with three different fuels: n-heptane, iso-octane and a mixture of 50% of n-heptane and 50% of toluene (in mass[37]). In the three cases, we keep constant the initial conditions of temperature and pressure, and we change the fuel/air equivalence ratio from 0.6 to 1.2.

In the three cases, there is a linear dependence for each fuel, that can be seen in the Fig. 10. The linear dependence of the equivalence ratio on the OH*/CH* chemiluminescence ratio can be described in the following way:

$$\left(\frac{\phi_{OH^*}}{\phi_{CH^*}}\right) = A_0 + A_1(Fr) \qquad (8)$$

where A_0, and A_1 are different parameters for each fuel. Fitting the data from Fig. 10 in the above way gives, Table 1:

For the three fuels shown in Fig. 10 (n-heptane and a mixture of n-heptane and toluene, which are surrogates of conventional diesel fuel), the dependence with equivalence ratio is linear. In the bibliography (see Higgins et al.[17]) we can find another similar correlation with an exponent of 2, for methane.

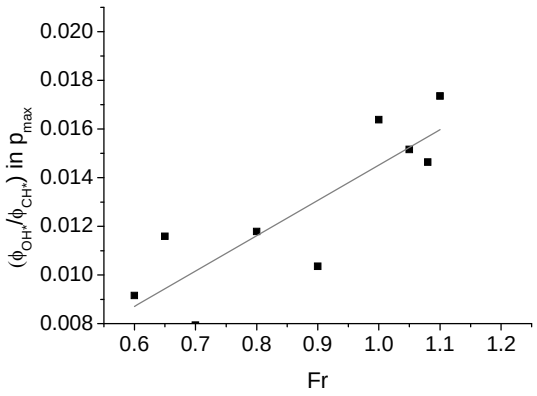

(i) n-heptane

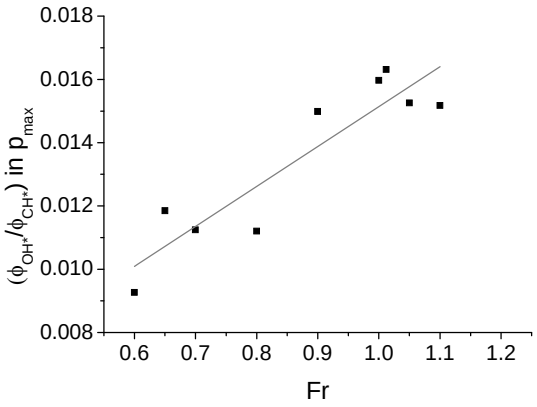

(ii) 50% n-heptane/ 50% toluene

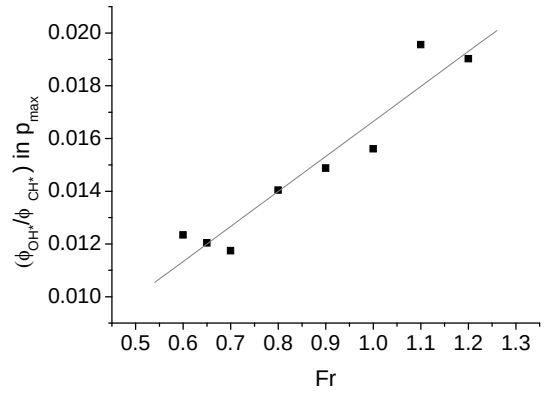

(iii) Iso-octane

Fig. 10. Relative OH* and CH* chemiluminescence signals as a function of the equivalence ratio in premixed combustions of (i)n-heptane. (ii) a mixture of 50% of n-heptane and 50% of toluene; and (iii) iso-octane, for stoichiometric equivalence ratio, an initial pressure of 0.8 MPa and initial temperature of 416 K of initial conditions.

3.5. Flame temperature and maximum pressure

In Fig. 11, the time at which maximum pressure is reached inside the CVCB is represented against the time at which the maximum CH* chemiluminescence is attained. It can be seen that both maximums are achieved at the same time. If the maximum CH* chemiluminescence is plotted against the flame temperature (see Fig. 11) it is possible to see that for the leanest equivalence ratio both maxima coincide and as the richness of the mixture increases both maximums are more separated. CH* chemiluminescence emissions are produced in the high temperature reactions which take place in the flame front of the combustion[1,31], as a consequence of the reactions which produce mainly OH* radicals, and precede the main heat release during the combustion. For this reason, CH* chemiluminescence emissions can be considered a good marker of the flame front position inside the CVCB.

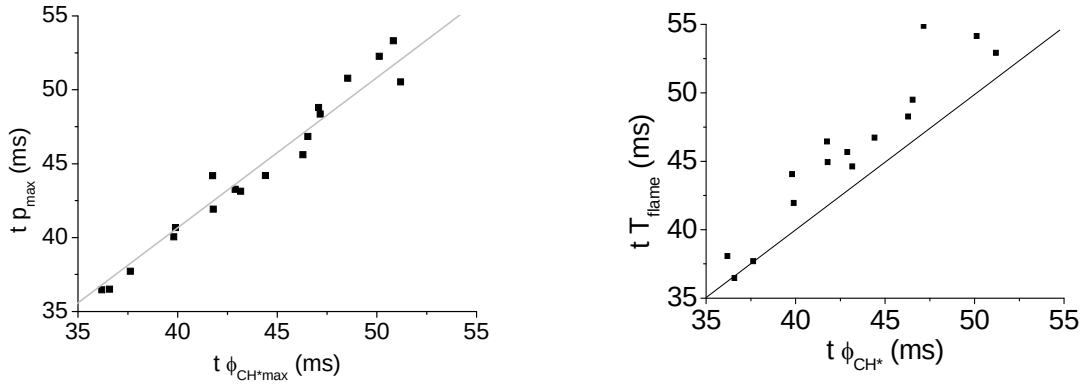

(i) Fr=1

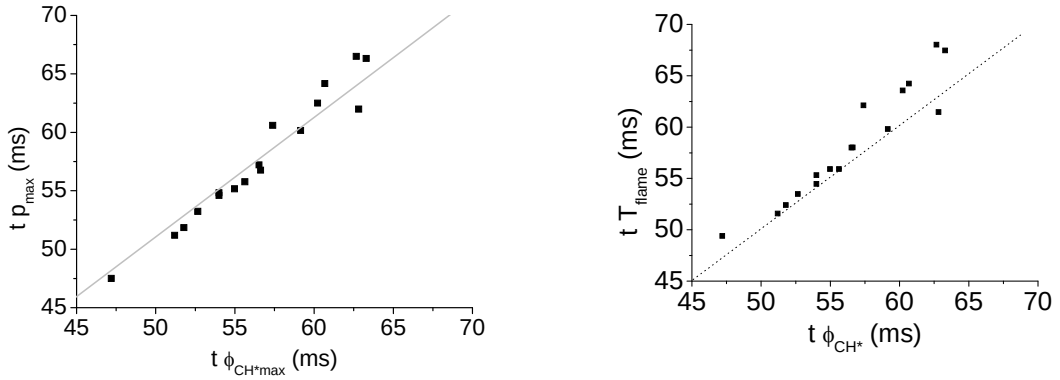

(ii) Fr=0.9

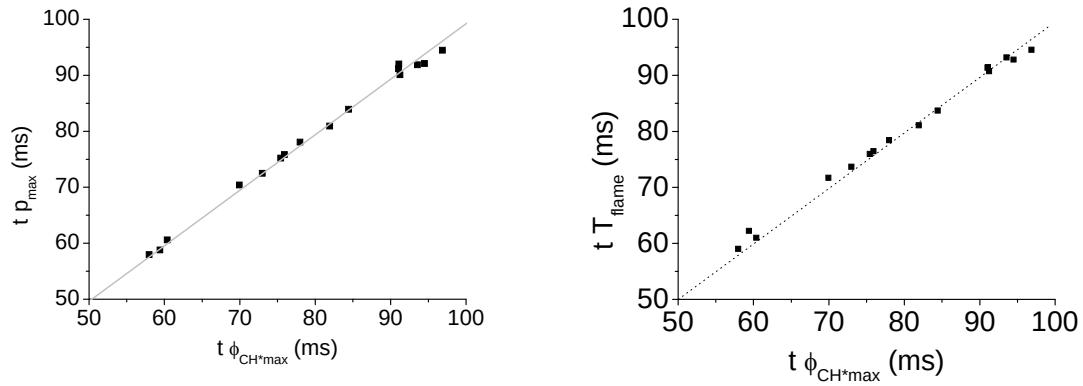

(iii) Fr=0.8

Fig. 11. Maximum pressure time and flame temperature time against the maximum CH* chemiluminescence emissions time in combustions of n-heptane with autoignition for different equivalence ratios, initial temperatures and pressures.

4. Conclusions

In this work, an experimental study of the OH* and CH* chemiluminescence emitted during the combustion of different primary fuels (n-heptane, toluene and iso-octane) at different initial conditions of pressure, temperature and equivalence ratio, under autoignition conditions, has been performed. The main conclusions of the experimental trends are summarised in the following:

OH* and CH* chemiluminescence emissions in n-heptane flames have been characterized in terms of morphology and absolute intensity. For both aspects (i.e., shape and intensity), the main dependence found is on mixture equivalence ratio (with a variation in intensity of one order of magnitude in the range of 0.8-1.) The second dependence is on temperature and the smaller dependence is on pressure.

OH* chemiluminescence can be used as a heat release marker of the combustion process, with its maximum emission peak coinciding with the highest rate of heat release inside the combustion bomb.

The ratio OH*/CH* of chemiluminescence signals have been studied with more detail, covering premixed flames of n-heptane/air, iso-octane/air, and a mixture of 50% n-heptane and 50% toluene/air combustions as a function of the equivalence ratio (0.6-1.1), for fixed initial pressure and temperature (0.8 MPa and 413 K). It has been found that the ratio of signals (OH*/CH*) is linearly proportional to the equivalence ratio for the three fuels considered.

ACKNOWLEDGMENT.

The authors of this paper would like to thank the Spanish Ministry of Science and Technology for the financial support of this research through the project TRA2007-67961-C03/AUT and the Regional Government of Castile and Leon through the funding for the GR203 Excellence Research Group. We also appreciate the help provided by Dr. Carot for the statistical design of experiments.

NOMENCLATURE

CVCB constant volume combustion bomb

F_r fuel/air equivalence ratio

h Planck constant

H enthalpy

HCCI homogeneous charge compression ignition

p pressure

PMT photomultiplier

Q heat

RoHR rate of heat release

T temperature (K)

V volume

GREEK:

F chemiluminescence (lm)

g adiabatic constant

$^{a}S^{a}$ determined excited estate

s standard deviation

n frequency

SUBSCRIPTS:

a	air
ad	adiabatic
aut	autoignition
b	burned
f	fuel
max	maxima
ub	unburned
*	excited radical

FIGURE CAPTIONS

Figure 1. Experimental facility. (i). Scheme of the experimental setup. (ii) Sketch of the optical accesses.

Figure 2. Diagnosis model outline.

Figure 3. Examples of some parameters obtained for a stoichiometric combustion of n-heptane with autoignition. Distinction between the combustion and the post-combustion (afterglow) zones. (i) Example of pressure, rate of heat release and combustion velocity. (ii) Example of temperature, OH* and CH* chemiluminescence emissions.

Figure 4. Autoignition intensity definition in a curve of stoichiometric n-heptane autoignition with pi=1.8 MPa and Ti=463K

Figure 5. Standard deviation of the experimental design proposed by a D-optimal type design of the n-heptane autoignition at different equivalence ratios 1, 0.9 and 0.8. (i) Fr=1. (ii) Fr=0.9. (iii) Fr=0.8.

Figure 6. Temporal evolution of the pressure (black line), OH* (grey line in the left plots) and CH* (grey line in the right curves) chemiluminescence in n-heptane premixed combustions with autoignition, for different equivalence ratios and for a fixed initial pressure and temperature of 2.0 MPa and 443 K, respectively. (i) Fr=1. (ii) Fr=0.9. (iii) Fr=0.8.

Figure 7. Pressure curve (black line) and OH* chemiluminescence (grey line) in n-heptane combustions with autoignition event, for different initial pressures and temperatures, for a fixed stoichiometric equivalence ratio.

Figure 8. Pressure curve (black line) and CH* chemiluminescence (grey line) in n-heptane combustions with autoignition event, for different initial pressures and temperatures, for a fixed stoichiometric equivalence ratio.

Figure 9. Maximum Rate of Heat Release time and maximum OH* chemiluminescence emissions in combustions of n-heptane with autoignition for different equivalence ratios, initial pressures and temperatures. (i) Fr=1. (ii) Fr=0.9. (iii) Fr=0.8.

Figure 10. Relative OH* and CH* chemiluminescence signals as a function of the equivalence ratio in premixed combustions of (i)n-heptane. (ii) a mixture of 50% of n-heptane and 50% of toluene; and (iii) iso-octane, for stoichiometric equivalence ratio, an initial pressure of 0.8 MPa and initial temperature of 416 K of initial conditions. (i) n-heptane. (ii) 50% n-heptane/50% toluene. (iii) Iso-octane.

Figure 11. Maximum pressure time and flame temperature time against the maximum CH* chemiluminescence emissions time in combustions of n-heptane with autoignition for different equivalence ratios, initial temperatures and pressures.

TABLES.

Table 1. Coefficients of the linear relation shown in Eq. 8, of the dependence between the ratio of OH* and CH* chemiluminescence and the equivalence ratio.

Fuel	**A_0**	**A_1**	**R^2**	**σ**
Iso-octane	$3.38\ 10^{-3}$	0.013	0.90	$1.50\ 10^{-3}$
n-heptane	0	0.015	0.98	$6.40\ 10^{-4}$
50% n-heptane/50% toluene	$2.52\ 10^{-3}$	0.013	0.82	$4.57\ 10^{-4}$

Table 1. Coefficients of the linear relation shown in Eq. 8, of the dependence between the ratio of OH* and CH* chemiluminescence and the equivalence ratio

REFERENCES

(1) Gaydon, A. G. *The spectroscopy of flames*; London Champan and Hall, 1974.

(2) Stojkovic, B. D.; Fansler, T. D.; Drake, M. C.; Sick, V. *Proc.Combust. Inst*. **2005**, 30, 2657-2665.

(3) Najm, H. N.; Paul, P. H.; Mueller, C. J.; Wyckoff, P. S. *Combust. Flame* **1998**, 113 (3), 312-332.

(4) Docquier, N.; Lacas, F.; Candel, S. Proc. *Combust. Inst.* **2002**, 29 (1), 139-145.

(5) Nori, N.; Seitzman, J. M. Proc. *Combust. Inst.* **2009**, 32 (1), 895-903.

(6) Aleiferis, P. G.; Hardalupas, Y.; Taylor, A. M. K. P.; Ishii, K.; Urata, Y. *Combust. Flame* **2004**, 136 (1-2), 72-90.

(7) Muruganandam, T. M.; Kim, B.H.; Morrell, M. R.; Nori, V.; Patel, M.; Romig, B. W.; Seitzman, J. M. Proc. *Combust. Inst.* **2005**, 30 (1), 1601-1609.

(8) Panoutsos, C. S.; Hardalupas, Y.; Taylor, A. M. K. P. *Combust. Flame* **2009**, 156 (2), 273-291.

(9) Tinaut, F. V.; Melgar, A.; Giménez, B.; Reyes, M. *Fuel* **2010**, 89 (3), 724-731.

(10) Ikeda, Y.; Kojima, J.; Nakajima, T.; Akamatsu, F.; Katsuki, M. Proc. *Combust. Inst.* **2000**, 28, 343-350.

(11) Dec, J.E.; Espey, C. Chemiluminescence imaging of autoignition in a DI Diesel engine. *SAE Technical Paper*, 982685, **1998**.

(12) Pastor, J.V.; Payri, R.; Gimeno, J.; Nerva, J.G. Energy Fuels 2009, 23, 5899-5915.

(13) Higgins, B.; McQuay, M. Q.; Lacas, F.; Candel, S. *Fuel* **2001**, 80 (11), 1583-1591. (14) Hardalupas, Y.; Orain, M.; Panoutsos, C. S.; Taylor, A. M. K. P.; Olofsson, J.; Seyfried, H.; Richter, M.; Hult, J.; Aldén, M.; Hermann, F.; Klingmann, J. *Appl. Therm. Eng.* **2004**, 24 (11-12), 1619-1632.

(15) Stevens, R.; Stone, R.; Walmsley, H. L.; Cracknell, R. *Proc. IMechE*, **2006**, 220, Part D: J. Automobili Engineering.

(16) De Leo, M.; Saveliev, A.; Kennedy, L. A.; Zelepuoga, S. A. *Combust. Flame* **2007**, 149 (4), 435-447.

(17) Ikeda, Y.; Kaneso, M.; Nakajima, T. Local A/F measurement by chemiluminescence OH*, CH* and C_2* in SI Engine. *SAE Technical Paper*, 2001-01-0919; **2001**.

(18) Higgins, B.; McQuay, M. Q.; Lacas, F.; Rolon, J. C.; Darabiha, N.; Candel, S. *Fuel* **2001**, 80 (1), 67-74.

(19) Dandy, D. S.; Vosen, S. R. *Combust. Sci. Technol*. **1992**, 82 (1), 131-150.

(20) Clark, B. L.; Thee, W. C. *Ind. Eng. Chem. Res*.**1926**, 18(5), 528-531.

(21) Clark, T. P. Studies of OH, CH, CH and C_2 radiation from laminar and turbulent propane-air and ethylene-air flames. *NACA Technical Note***1958**, 5,4266.

(22) Docquier, N.; Belhalfaoui, S.; Lacas, F.; Darabiha, N.; Rolon, C. Proc. *Combust. Inst.* **2000**, 28 (2), 1765-1774.

(23) Price, R. B.; Hurle, I. R.; Sugden, T. M. *Symposium (International) on Combustion* **1968**, 12 (1), 1093-1102.

(24) Withrow, L. and Rassweiler, G. M. Ind. Eng. Chem. 1931, 23 (7), 769-776.

(25) Hultqvist, A.; Christensen, M.; Johanson, B.; Franke, A.; Ritcher, M.; Aldén, M. A study of the homogeneous charge compression ignition combustion process by chemiluminescence imaging. *SAE Technical Paper*, 1999-01-3680; **1999**.

(26) Habo-Mohamed, A. R. *Optical sensors for flame progress monitoring in spark ignition engines*. Master-thesis, University of Leeds, Mechanical Engineering Department, 1990.

(27) Gaydon, A.G. and Wolfhard, H.G. *Flames: Their structure, radiation and temperature*. Champan & Hall: London, 1979.

(28) Dubreuil, A.; Foucher, F.; Mounaïm-Rouselle, C. *Energy Fuels* **2009**, 23, 1406-1411.

(29) Mancaruso, E. and Vaglieco, B.M. *Experimental Thermal and Fluid Science* **2006**, 34 (3), 346-351.

(30) Mancaruso, E.; Merola , S.S.; Vaglieco, B.M. Extinction and Chemiluminescence measurements in CR DI Diesel Engine Operating in HCCI mode. *SAE Technical Paper*, 2007-01-0192; **2007**.

(31) Hernandez, J. J.; Sanz, J.; Benajes, J.; Molina, S. *Fuel* **2008**, 87 (6), 655-665.

(32) Horrillo, A. *Utilization of multi-zone models for the prediction of the pollutant emissions in the exhaust process in spark ignition engines*. PhD Thesis, University of Valladolid (in Spanish), 1998..

(33) Reyes, M. *Characterization of the combustion and auto-ignition processes of liquid fuels in homogeneous mixtures for using in internal combustion engines running in HCCI mode*. PhD. Thesis, University of Valladolid, Spain (in Spanish), 2008.

(34) Tinaut, F.V.; Melgar, A.;Horrillo, A.J. Utilization of a quasi-dimensional model for predicting pollutant emissions in SI engines. *SAE Paper*,1999-01-0223; **1999**.

(35) Krishnamachari, S.L.N.G. and Broida, H. P. J. *Chem. Phys*. **1961**, 34 (5), 1709-1711.

(36) Becker, K. H. and Kley, D. Chemical Physics Letters **1969**, 4 (2), 62-64.

(37) Lee, S. W.; Tananka, D.; Kusaka, J.; Daisho, Y. *JSAE Review* **2002**, 23 (2), 195-203.

(38) Devriendt, K.; Van Look, H.; Ceursters, B.; Peeters, J. *Chemical Physics Letters* **1996**, 261 (4-5), 450-456.

(39) Kirkbright, G.F. and West, T.S. *Applied Optics* **1998**, 7 (7), 1305-1323.

(40) Fields, M.; Zheng, J.; Qian, S.X.; Kindlmann, P.J.; Swindal, J.C.; Acker, W.P. Single-shot temporally and spatially resolved chemiluminescence spectra from and optically resolved chemiluminescence spectra from an optically accessible SI engine. *SAE Technical Paper*, 950105; **1995**.